EXPLICIT ANALYSIS OF THE LATERAL MECHANICS OF WEB SPANS

By

B. Fu, R. Markum, A. Reddy, S. Vaijapurkar, and J. K. Good
Oklahoma State University
USA

ABSTRACT

All previous analyses of webs being steered through process equipment have required enforcement of assumed boundary conditions. An example is the normal entry boundary condition which has been employed in many web/roller analyses.

Explicit finite element analyses show much promise for studying all types of web handling problems. The primary benefit of this type of analysis is that only very basic assumptions are required, average web velocity and tension for example. Beyond this the interaction of webs with rollers are governed entirely by forces of contact and friction that develop between the web and rollers. Conditions of stick and slip are possible. Additional benefits include the ability to study web deformations and stresses which may result in the development of boundary conditions that can be employed in models that are computationally less expensive.

This paper will focus on a study of the lateral behavior of a web transiting a set of rollers in a process machine, one of which will be misaligned. The misalignment will be increased until there is interaction with an upstream span, a phenomena that has been previously called moment interaction. Any steering of a web laterally in a process machine produces reactions that must be resolved as frictional forces between the web and rollers. Thus the slightest misalignment of a roller will induce some slippage between the web and an upstream roller. That slippage will become gross as the degree of misalignment increases until it migrates around the upstream roller and induces lateral deformation in the upstream span. These phenomena will be studied and results will be compared to experiments. Finally an assessment of potential boundary conditions will be made.

INTRODUCTION

The assumptions made for the analysis of single span web systems may not be valid when multiple span web systems are taken into account. For example, the cantilever support assumed by Shelton [1] at the upstream roller in a single span would require

infinite friction between the web and the upstream roller as the web exits the roller. Since infinite friction cannot exist, some slippage will result. This condition is shown in Figure 1(a) for a two span web system. Three rollers are shown in a single plane but in reality the web wraps around each roller 90°. Whenever Roller 3 (R3) is misaligned, a bending moment is developed in the entering Span B. The bending moment is maximum as the web exits Roller 2 (R2) and decreases linearly to zero as the web approaches R3 [1]. The value of the bending moment in the web at the exit of R2 increases with the increased misalignment of R3. This moment must be reacted by frictional forces associated with slippage of the web on R2. When the moment is small this slippage will occur near the exit of the web from R2 and the lateral deformations will be confined to Span B as shown in Figure 1(a). As the moment becomes larger the slippage will occur over a larger portion of the total contact area between the web and R2. There is a limit to the moment that can be reacted by friction which is called the critical moment, M_r. Closed form solutions to calculate the critical moment have been developed and reported by Dobbs and Kedl [2], Good [3] and Shelton [4] using different assumptions and models. In these references whenever the misalignment of R3 produces a moment in the web at the exit of R2 that surpassed M_r, the condition of moment transfer from Span B into Span A begins. Once this occurs there are bending moments and lateral deformations introduced into web Span A. This behavior is shown in Figure 1(b). The machine direction (MD) tension distribution at each roller associated with the misalignment and hence the induced bending moments is also shown.

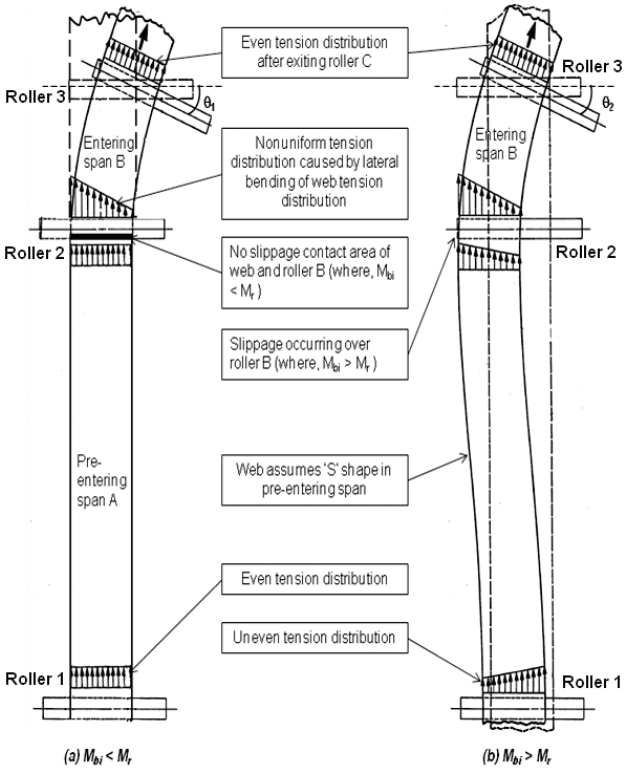

Figure 1 – Schematics of lateral deformation and tension distribution before and after slippage at R2 due to misalignment at R3.

The focus of this research is to study the transfer of moment from one span (entering span) to an upstream span (pre-entering span). The moment transfer is induced by a misaligned downstream roller in the entering span. In the laboratory Laser Doppler Velocimeters (LDV) were used to measure a change in MD strain across the web width due to the misalignment. In-situ moment values in the moving web spans could be inferred from these strain differences. To study the moment transfer, moment values were inferred using this method in several MD locations in two web spans for varied levels of misalignment at the downstream roller. Lateral displacements of the web were also measured using Keyence edge sensors. The roller misalignment was increased in steps until moment started transferring into the pre-entering span. The experiments were designed and the measurements were conducted by Reddy [5].

Unlike the previous finite element (FE) simulations on misalignment [6], commercial FE software Abaqus/Explicit [7] was employed in this work. Explicit FE analysis involves the solution of the equations of motion through time:

$$[M]\{\ddot{u}\} + [C]\{\dot{u}\} + [K]\{u\} = \{F(t)\} \qquad \{1\}$$

where [*M*], [*C*], and [*K*] are the mass, damping, and stiffness matrices formed using the finite element method. $\{\ddot{u}\}$, $\{\dot{u}\}$ and $\{u\}$ are the acceleration, velocity, and displacement vectors through time that form the response of the system due to applied loads *F* and constraints that can also vary with time. In the simulations of this study, the web and rollers were modeled. The simulation was started by restraining the downstream web end and then applying a uniform tension at the upstream end of the web model. Contact pressure formed between the web and roller surfaces during this step. Next the downstream end of the web is ramped to a constant level of velocity. At this point in the simulation we have a web with a constant tension travelling about aligned rollers. In the next step a roller is misaligned. The web attempts to steer into the misaligned roller so that the directions of velocity of the web surface and the misaligned roller can match, due to assumed Coulomb friction. If the velocities can match in direction and magnitude, normal entry of the web to the downstream roller may result. In the remainder of the simulation the web achieves a steady state lateral deformation. When this occurs the output can be compared to available test data. In this study the test data used for comparison will include lateral deformations at discrete MD locations and measured internal moments at several locations.

No lateral deformation or slope of the web was enforced as a constraint at any roller in these simulations. The lateral tracking of the web over the rollers is dictated only by the friction forces that develop between the web and rollers.

EXPERIMENTAL PROCEDURE

Good *et al.* [8] demonstrated how the LDV can be used to measure a strain change between in two points in a web. In that publication the change in strain was measured down the length of the web such that a change in web tension could be inferred. In this study a change in strain across a web width will be measured from which the internal moment in the web can be inferred. The Laser Doppler Velocimeter is a device that is capable of measuring velocity directly. Most of these devices output a TTL (Transistor Transistor Logic) pulse train from which the length of a moving strained or unstrained surface can be inferred, similar to the output of an encoder which might touch a web via a contact wheel. The method requires that the moving surface be opaque and have some

surface roughness. The LDVs (Model LS200) used herein were produced by BETA LaserMike[1].

A set-up of two LDVs was used to acquire the data induced in web spans due to a misaligned downstream roller. The LDVs were mounted above the web span side by side in the cross machine direction (CMD) to measure the length of the web moving beneath them as shown in Figure 2. The length of deformed web measured by the LDVs was used to calculate a relative strain across the web width. When the downstream roller is aligned, the difference of pulses from the LDVs (LDV_a - LDV_b) must be zero because of zero bending moment in the web. Whenever there is some misalignment in a span, one edge of the web becomes longer when compared to other edge due to the bending moments and strains that result. The difference in the counts output by LDVs is directly proportional to the bending strain in the web at an MD location.

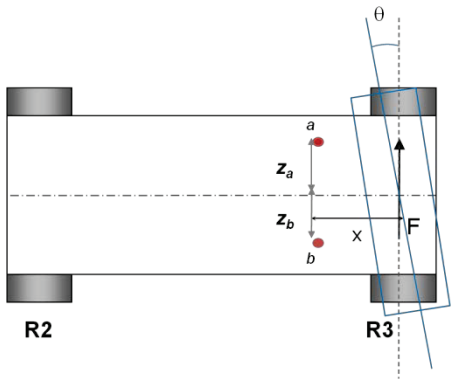

Figure 2 – Schematic plot of LDVs install positions

The LDVs were set at various 'x' positions in the spans where moments were intended to be measured, see Figure 2. Each LDV was made to shoot at a distance of 63.5 mm above and below the central axis of the web, thus the distance between the two LDV measurements is 127 mm. The strains at locations *a* and *b* and their difference will be:

$$\varepsilon_a = \frac{Mz_a}{EI} + \frac{T}{AE}, \varepsilon_b = \frac{Mz_b}{EI} + \frac{T}{AE}, \varepsilon_a - \varepsilon_b = \frac{M(z_a - z_b)}{EI} \quad \{2\}$$

Where M is the moment, T is the web tension, E is Young's modulus, I is the area moment of inertia, A is the cross sectional area and z_a and z_b are the distances shown in Figure 2. Thus the moment can be inferred experimentally using:

$$M = EI\frac{\varepsilon_a - \varepsilon_b}{z_a - z_b} \quad \{3\}$$

where,

[1] Beta LaserMike Americas, 8001 Technology Blvd., Dayton, OH, 45424 USA

$$\varepsilon_a - \varepsilon_b = \frac{LDV_a - LDV_b}{LDV_a} \qquad \{4\}$$

The LDVs yield an output of 1000 TTL pulses per 0.3048 m (1 ft) of passing web or 100,000 pulses for 30.48 m (100 ft) of web. At each 'x' position in the span, ten measurements were made as 30.48 m of web were allowed to pass the LDVs. This length of web was chosen to increase the precision of the strain difference measurement as determined by expression {4}. This will produce an accuracy of approximately 1/100,000 or 10 μS which was found to be satisfactory in this study. Greater accuracy could have been obtained by making measurements over yet longer lengths of web but to achieve that accuracy would require the web and the operating parameters to remain constant while the length of web selected passed the measurement site.

To study the moment transfer in a multi-span web system, a machine (test rig) was needed which would allow the misaligning of a downstream roller and letting the moments transfer upstream into the pre-entering span. To investigate moment distribution in web spans, the LDVs needed to move to multiple test locations in the entering span, around the upstream roller (R2) and in the pre-entering span while maintaining the required standoff distance (304.8 mm). A schematic showing dimensions and locations of edge sensors and LDVs is shown in Figure 3. The finished assembly of the new test rig and the winder setup is shown in Figure 4.

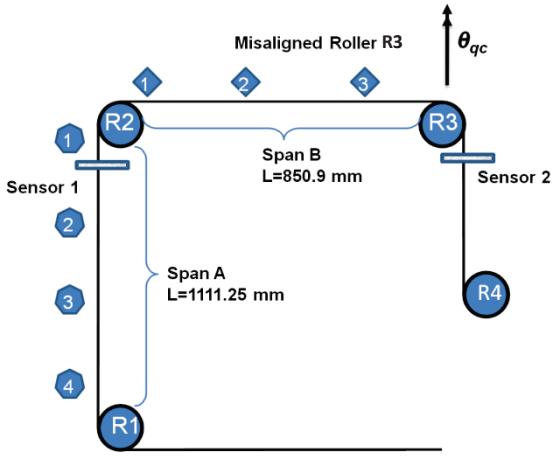

Figure 3 – Schematic plot of test rig design

In this design, the web is passes from the pre-entering Span A around R2 into entering Span B. The LDVs were positioned on a rotating arm as shown in Figure 4 which slides on a set of rails traversing Span A, R2 and Span B. The misalignment of R3 is precisely set with the help of a micrometer and was measured using a linear variable differential transformer (LVDT). R3 sits on a carriage that slides on the horizontal rails to adjust the desired length of Span B. A web guide was installed just before the web enters the pre-entering Span A. The web guide ensured that the lateral web position was maintained at the entry of the test section (Spans A and B). At the right in Figure 4 an unwind/rewind system is shown that was responsible for maintaining the web tension and velocity at a constant level during a test. Note the two Keyence edge sensors (LS-3100)

which were used to measure the lateral deformation of the web near the exit of Span A and after the web exits Span B. A National Instruments 6602 counter/timer was used to simultaneously acquire the TTL pulses from the LDVs. A LabVIEW™[2] VI triggered two counters that began counting pulses from LDV_a and LDV_b. Whenever one of the two counters reached 100,000 pulses the counters were triggered off. The count values and the count difference were stored, the counters were cleared, and the counters were triggered on again in a repeating cycle. The count difference could then be used in expressions {3} and {4} to establish the moment. Ten cycles of LDV data were acquired at any one MD location and the results were averaged.

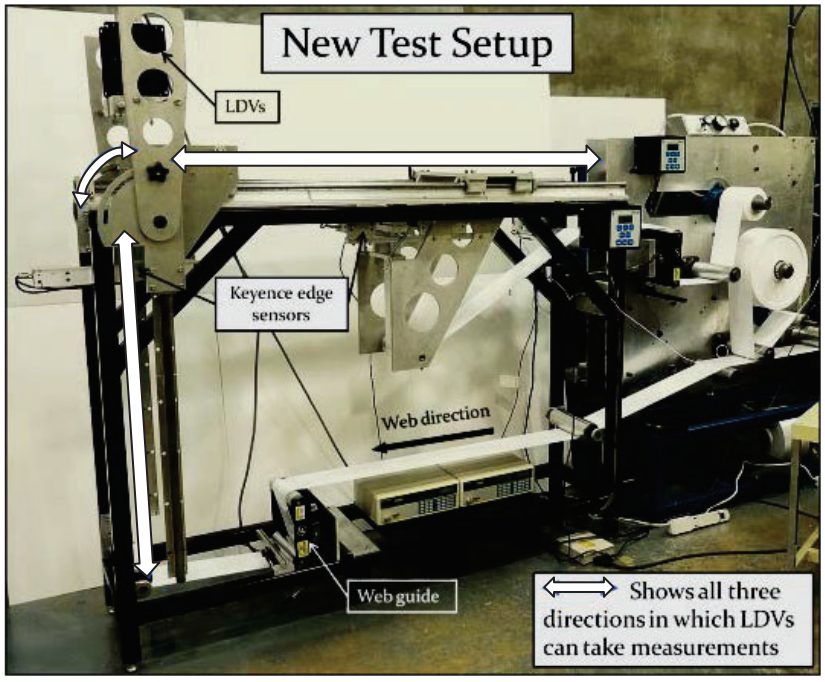

Figure 4 – Finished assemble of the new test rig and the winder setup

[2] LabVIEW is a trademark of National Instruments Corporation, Austin, TX, USA.

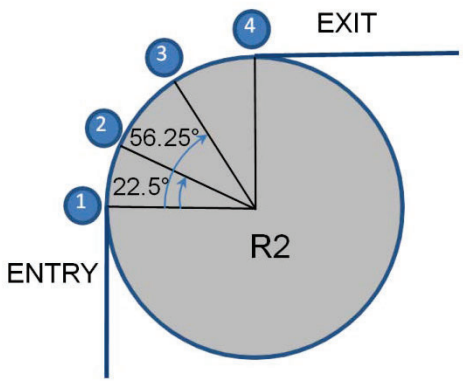

Figure 5 –Schematic diagram showing test locations on R2.

Using this apparatus, measurements were recorded at four locations in the pre-entering Span A (heptagon symbols) and three locations in entering Span B (diamond symbols) as shown in Figure 3. In addition, LDV measurements were taken at four locations on R2 (circle symbols) as shown in Figure 5. Table 2 provides all of the positions at which LDV data was recorded. The second column includes the locations in the pre-entering span starting from the furthest one from entry point to R2 (location 1). The third column shows the locations starting from entry point to R2. The last column gives the locations in entering span starting from the nearest one to exit point (location 4). As shown in Figures 3 and 4, the two Keyence edge sensors were installed to measure the lateral displacements at 165.1 mm before web enters R2 and 101.6 mm after web exit from R3 respectively. Five different misaligned angles were used in the tests: 0.074°, 0.223°, 0.446°, 0.502° and 0.558°. Based on the estimation method reported by Good 3, moment transfer should begin when R3 is misaligned 0.446°.

LDVs locations	Distance from entry point 1 (mm) in pre-entering span	Distance from entry point 1 (mm) on R2	Distance from exit point 4 (mm) in entering span
1	838.2	0	50.8
2	558.8	14.96	381.0
3	279.4	37.34	762.0
4	50.8	59.84	

Table 2 – Data taken locations in pre-entering and entering spans and on R2

FINITE ELEMENT SIMULATION MODEL

A four-roller FE model was setup to model Spans A and B in the test setup using Abaqus 6.9 [7] as shown in Figure 6. The modeled web has the same dimensions as the web that Reddy used in the measurements, which are 152.4 mm (6 in) in width and 0.0508 mm (0.002 in) in thickness. An oriented polyester film was employed. Reddy measured Young's modulus (E) for this web at 3.93 GPa and Poisson's ratio (ν) was set to 0.3. (The free web span length modeled starting from Roller 1 (R1) and moving to the upstream end of the web is more than three times the entering span length (850.9 mm) between R2 and R3.) This length of web needed to travel through the entering span to

allow steady state lateral behavior to be achieved. The dynamics of web transient lateral behavior can often be characterized as a first order system because the inertial forces $([M]\ddot{w})$ are small due to a small web mass when compared to the damping forces $([C]\dot{w})$ and the forces due to deformation ($[K]w$). The inertial forces become yet smaller as the system approaches steady state deformation. The transient response of a single degree of freedom first order system due to a step input in external force ($[F_o]$) is:

$$w = \frac{[F]}{[K]}(1 - e^{-[K]t/[C]}) = w_\infty(1 - e^{-t/\tau}) \qquad \{5\}$$

In this case the step input is the misalignment of R3, but this will introduce steps in moment and shear in Span B and the system response will be similar to that given in expression {5}. The time constant τ in a single web span is the time required for the web to move through the span. After the step disturbance in misalignment and after three span lengths of web have passed, expression {5} predicts that the lateral deformation (w) would be approaches 95% of the final value (w_∞). After four span lengths of web have passed, the lateral deformation will have reached 98.2% of the final value. This rationale was used to define the length of the incoming web prior to R1. Once moment transfer begins the time constant will be longer than the time required for the web to transit the distance between R2 and R3. To address this issue, a longer free span was modeled prior to R1 for larger misaligned angles where moment transfer would occur. In these cases the response of the web (lateral deformation and velocity) entering R3 is reviewed through time to ensure that steady state behavior has been achieved.

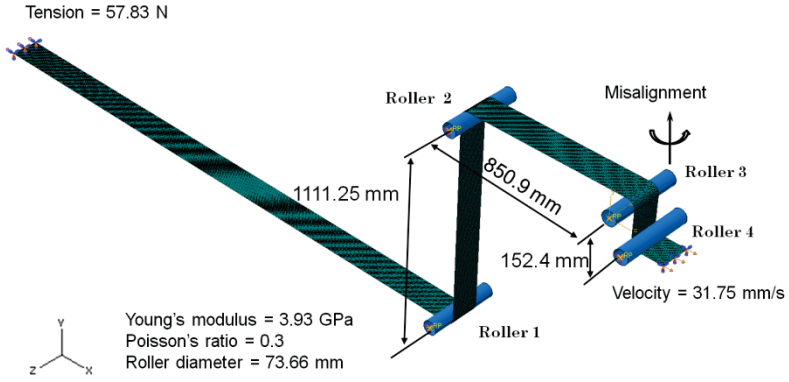

Figure 6 –Four-roller FE model set up

During the simulations, R3 was misaligned at a specified angle as shown in Figure 6 which induced lateral motion in the web. In these simulations, the web was given a velocity of 31.75 mm/s at the downstream end. A tension load of 57.83 N, the same as that used in the experiments, was applied on the upstream end of the web. Both this velocity and load were brought from zero to their final values linearly with time at the beginning of the simulation and then kept constant through the remainder of the simulation. In the experiments, R1 and R3 had high coefficient of friction coatings (Dow 236). Although lab tests have shown that these coatings can produce friction coefficients in excess of 4, the friction coefficients at R1 and R3 was set to 0.9 in the simulations.

This was done because Coulomb friction coefficients in excess of unity can produce odd model behaviors. As long as the friction coefficients are set high enough to confine the transient behavior to Spans A and B between R1, R2, and R3 the simulation and test behaviors should be similar. Reddy measured a friction coefficient of 0.33 between the aluminum roller surfaces and the polyester web and this friction coefficient was assigned to the contact properties for R2 and Roller 4 (R4).

Since the aluminum rollers are much harder and stiffer than the web material, the rollers were modeled as analytical rigid parts. In Abaqus, analytical rigid parts do not require meshing and are continuously defined geometry shapes. The importance of this is related to the contact algorithms used by Abaqus. The errors in computing contact pressure and slippage for a discrete web in contact with an analytical surface are less than the errors for a discrete web in contact with a discrete roller surface. The web material simulated in this work is a polyester plastic film. Membrane elements (M3D4R) [7] were used to generate the web model in these simulations. The membrane elements have two particular characteristics: they are surface elements that only transmit in-plane forces (no moment); and they have no bending or transverse shear stiffness. Therefore, the only nonzero stress components in the membrane elements are those components parallel to the middle plane of the element. In the other words, the stress state of membrane is plane stress. Since there is no transverse shear of membrane, the components of the deformation gradient $\mathbf{F} = \partial\mathbf{u}/\partial\mathbf{X}$ are defined as:

$$F_{3\alpha} = \mathbf{e}_3 \cdot \frac{\partial \mathbf{u}}{\partial X_\alpha} = 0, \text{ and } F_{\alpha 3} = \mathbf{e}_\alpha \cdot \frac{\partial \mathbf{u}}{\partial X_3} = 0 \qquad \{6\}$$

in Abaqus. As a result, there is no out-of-plane deformation if only in-plane forces are applied. Because membrane elements have fewer degrees of freedom than shell elements, the simulations would execute faster for a given mesh density and the output results have been found to exhibit less noise than simulations employing shell elements.

SIMULATION AND EXPERIMENTAL RESULTS

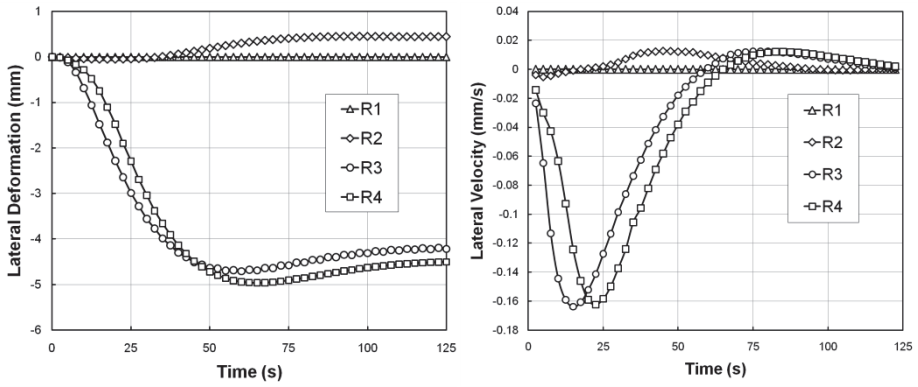

(a) (b)

Figure 7 – (a) Web Lateral displacements at the entry point of each roller; (b) Calculated velocity at the entry point of each roller.

Simulations have been done using the model created with consideration of dynamic equilibrium. To explore the behavior of moment transfer, several direct output variables from simulations have been studied, the lateral displacements and MD stresses are examples. The slope of the lateral deformation, velocity and moment distribution can be calculated using the lateral displacements and MD stresses. To demonstrate that steady state conditions have been reached, the lateral displacements of the web acquired at the entry points of the four rollers and the corresponding calculated velocities are shown in Figure 7. This data was collected on the web centerline (the elastic axis). At the start of the simulation the lateral deformations of the web are all zero entering each of the four rollers. As the simulation progresses note that the lateral deformation remains zero as the web enters R1. This is an indication that the moment interaction has been confined to Spans A and B. As the simulation progresses note the positive lateral deformation of the web at R2 followed by negative deformations at R3 and R4. The signs of these deformations are with respect to the coordinate axes shown in Figure 6 where a positive misalignment angle is shown. The shape of the deformed web is consistent with the illustration of lateral deformation under moment transfer conditions shown in Figure 1(b). The displacements reach steady state after about 120 seconds for this case (0.446°) as shown in Figure 7(a). As shown in Figure 7 (b), the lateral velocities of the web before entering each roller converge to zero after about 120 seconds. This means the web is not going to move laterally anymore and that steady state behavior has been achieved. The results presented hereafter were harvested from the last step of simulations.

The lateral displacements from the simulation output can be studied and compared directly with the lateral displacements measured during tests. Reddy measured these lateral displacements [5] and the data is shown in Tables 3 & 4 for five misalignment angles of R3. The lateral displacements from the five simulations along the centerline of the web are shown in Figure 8. The experimental results agree with the simulation results very well except for the case where R3 was misaligned 0.074°. The lateral displacements are relatively small in this case and the difference is small (around 0.127 mm). These deformations were measured several times (N>100) while the LDV data was being acquired. The standard deviation of this data was typically 0.06 mm. The accuracy of the Keyence LS 3100 sensor is specified as 3 μm. The standard deviation of the edge deformation data is high compared to the accuracy of the instrument and thus it must be concluded that the standard deviation of the data is a measure of the slit edge quality. Also shown are the lateral deformations that were calculated using the closed form expressions developed by Good [3] which also agree well with the results from the Abaqus simulations and the experimental data. To determine whether normal entry was achieved the slopes were calculated using the lateral displacements shown in Figure 8 and overlaid in the charts of Figure 8. The slopes were calculated using a finite difference method to estimate the first order differentiation of lateral displacements with respect to the MD coordinate. The slope is not a direct output for the membrane element because an out-of-plane rotation (in fact any rotation) is not a defined degree of freedom. The study of boundary conditions of the web entering and exiting R2 and R3 is one of the objectives of this work. Vertical lines have been added in Figure 8 to help interpret the locations of where the web enters and exits R2 and R3 and to aid in determining the lateral displacements and slopes of web at these locations.

Lateral deflection (Sensor 1)	Misalignment angle (°)				
	0.074	0.223	0.446	0.502	0.558
Experimental (mm)	0	0	0.04826	0.7188	0.894
Abaqus (mm)	5.72e-5	6.045e-3	0.4161	0.7137	1.069
Good 3 (mm)	0	0	0	0.460	0.9195

Table 3 – Lateral deflection measurement from upstream edge sensor

Lateral deflection (Sensor 2)	Misalignment angle (°)				
	0.074	0.223	0.446	0.502	0.558
Experimental (mm)	-0.6706	-2.2936	-4.270	-4.7346	-5.1359
Abaqus (mm)	-0.8026	-2.4409	-4.5034	-4.7803	-5.0394
Good 3 (mm)	-0.7899	-2.3774	-4.7549	-4.8616	-4.9682

Table 4 – Lateral deflection measurement from downstream edge sensor

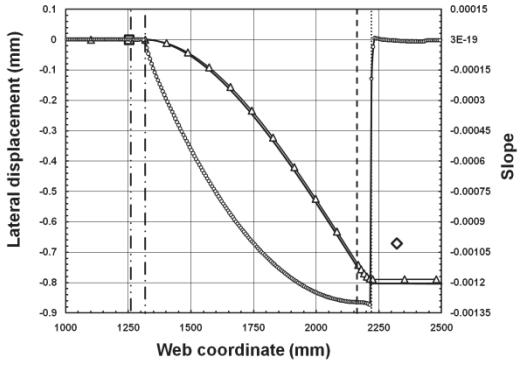

(a)

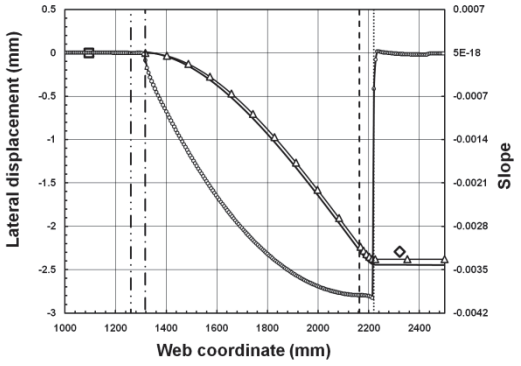

(b)

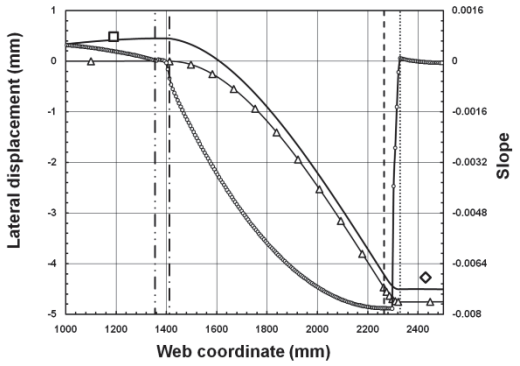

(c)

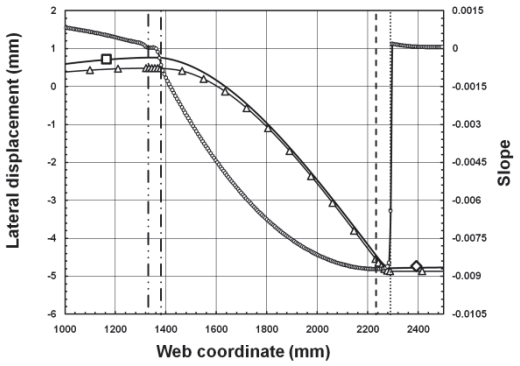

(d)

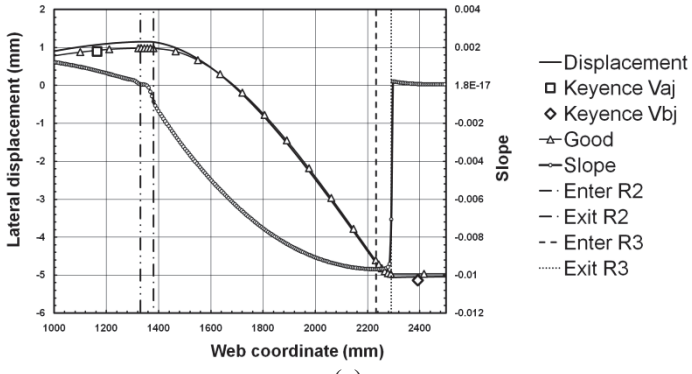

(e)

Figure 8 – Lateral displacement comparison between simulations and experiments, and the calculated slope curve for each misaligned angle: (a) 0.074° (0.00129 radians) (b) 0.223° (0.00389 radians) (c) 0.446° (0.00778 radians), (d) 0.502° (0.00876 radians) and (e) 0.558° (0.00974 radians).

From Figure 8, it is apparent that the web exits R2 with zero lateral displacement and small negative slope in the 0.074° and 0.223°. This slope becomes negative before the

web exits R2 and is an indication of local web slippage at the exit of R2. The negative slopes increase at the exit of R2 as the misalignment at R3 increases shown in Figure 8 (c), (d), (e). Moment transfer was predicted to begin when R3 was misaligned 0.446° using closed form expressions from Good [3]. It is obvious that moment transfer has already begun at this misalignment as shown in Figure 8 (c). The lateral displacement of the web entering R2 is no longer zero for this or the larger misalignment angles as shown in Figures 8 (d) and 8 (e). In all cases the web moves laterally after it exits from R2 and the lateral displacements increase (negatively) nonlinearly with respect to the MD. The lateral displacements become more linear as the web approaches R3 in all cases. After exiting R3, the lateral displacement of the web remains at a constant value. The web achieved normal entry to R3 in all five cases. Note the web slope matches the misalignment of R3 in each case in Figure 8. As the web transits R3 the slope remains nearly constant until the exit zone is reached where a transition to web twist occurs.

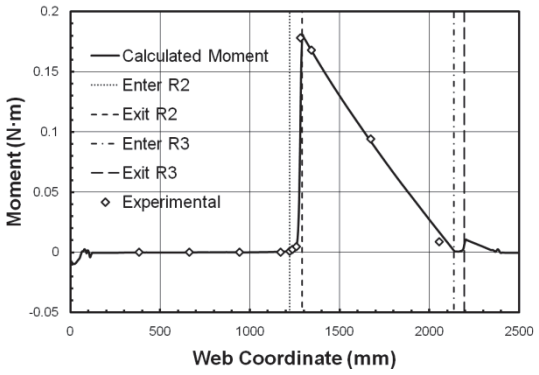

(a)

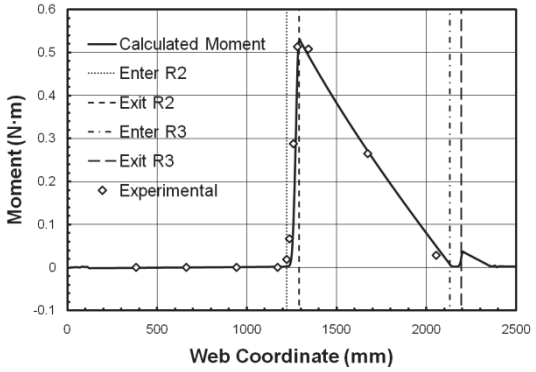

(b)

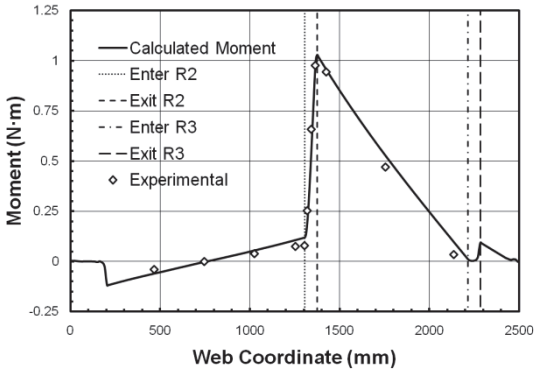

(c)

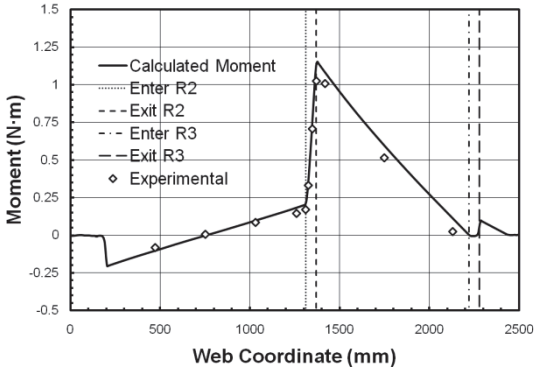

(d)

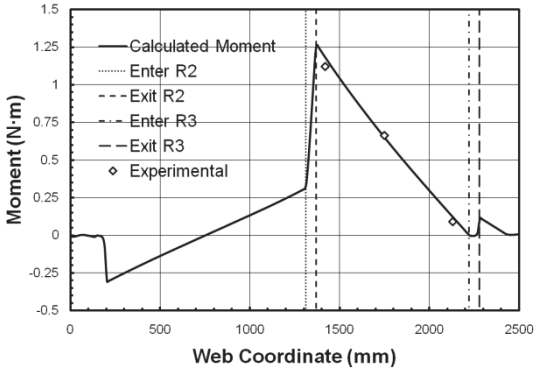

(e)

Figure 9 – Moment comparison between simulations and experiments: (a) 0.074° (b) 0.223° (c) 0.446°, (d) 0.502° and (e) 0.558°.

To further investigate moment transfer and compare with experimental results, the calculated moments using simulation outputs and experimental results in the web spans for each case was plotted in Figure 9. Due to a measurement limitation, the data were

only available in the entering Span B for the 0.558° case. In the simulations, MD stress values were harvested for each integration point in each element in the CMD at a particular MD location. These stresses were then used to estimate the internal moment in the web at that MD location using the expression:

$$M = \int \sigma_{MD} z dA = \sum_{i=1}^{n} \sigma_{MDi} z_i A_i \qquad \{7\}$$

where σ_{MDi}, z_i, and A_i are the MD stress levels at the integration points, the distances between the integration points and the elastic axis, and the elemental areas, respectively.

As mentioned previously, the LDV measurements used to infer the internal moment were taken at different locations in the pre-entering Span A, the web on R2 and the entering Span B. The inferred moments are shown as discrete data points at the MD locations where the LDV data was collected (refer to Figures 3, 5 and Table 2). Each inferred moment shown as a data point was the mean of 10 sets of LDV measurements. The standard error of this data in units of the inferred moment was 0.01 N-m. The simulation results agree with experimental results very well at each point. The moment reaches its peak value at the exit of R2 and then decreases almost linearly as the web approaches R3 in the entering Span B. Finally, the moment decreases to zero when the web arrives at the misaligned R3 and is consistently zero on the roller until the web exits from it. It is worthy to note that the moment at the entry point of the web to R3 is not exactly zero, but it is a very small value. This provides additional evidence to support Shelton's assumption [1] of zero moment at the entry of the misaligned downstream roller.

To further explore the boundary conditions, the curvatures in Spans A and B were studied. The curvature was determined using a finite difference estimate of the second derivative of the lateral displacements of the elastic axis from the simulations with respect to the MD coordinate. The curvature and the moment are related by the well-known Bernoulli-Euler relationship for small deformations:

$$\frac{1}{R} = \frac{d^2 w}{dx^2} = \frac{M}{EI} \qquad \{8\}$$

where *1/R* is the web curvature, *R* is the radius of curvature, and *w* is the lateral deformation of the web. Thus the curvature could also be inferred by using expression {8} in conjunction with the moments that were shown in Figure 9. The curvatures derived by the two different means are shown in Figure 10. The Bernoulli-Euler expression is considered valid for cases where the shear deformations are small and where the beam deformations are small. For the span ratio of Span B (850.9/152.4=5.6) the shearing deformation accounts for less than 5% of the total lateral deformation. The maximum lateral deformations in this study are two orders of magnitude smaller than the span length of Span B (5.08/850.9=0.006). Thus the Bernoulli-Euler expression should be valid. As shown in Figures 9 and 10, the web enters roller R2 with zero curvature for cases with no moment transfer. These curvatures were not equal to zero after moment starts transferring. As the web exits R2, the curvature jumps to a peak value (negatively) suddenly, and then drops back to around half of the peak value (except 0.074° case) quickly with the web moving away from R2. In all five cases, the web curvature decreases almost linearly between R2 and R3. With the web entering R3 normally as stated previously, the web curvature drops to zero at the location near to the web entry of

R3. On the misaligned roller, the curvature remains constant as the web is wrapping the roller, followed by a small jump due to the twist of the web as it exits R3. This small jump was diminished in a simulation where the exit span of R3 was lengthened.

The deviation of the curvature inferred from slope and from bending moment was studied further. The Euler-Bernoulli expression {8} requires plane sections to remain plane after deformation. If the deformations were large expression {8} should be expanded to:

$$\frac{1}{R} = \frac{d^2w/dx^2}{[1+(dw/dx)^2]^{3/2}} \qquad \{9\}$$

Expression {9} was used to develop the curvature for the 0.446° case using the lateral deformations produced by the simulation. That curvature and the curvature calculated using moments inferred from MD stresses {7} are shown in Figure 11. If the curvature calculated using expression {8} from Figure 10c is compared with the curvature in Figure 11 from expression {9} there is no distinguishable difference and provides validation of the small deformation assumption. In the pre-entering and entering spans, both methods shown in Figure 11 show a linear characteristic and agree with each other very well. The two methods yield nearly zero curvature as the web enters R3, which is consistent with the previous conclusion. The only significant differences occurs when the web exits rollers R2 and R3. To investigate the planarity of the web after deformation, the MD displacements across the web width are shown at three different selected locations in Figure 11. The MD displacements indicate a planar deformation midway in the entering span. When the web exits from R2 and R3, the MD displacements along CMD are shown to be non-planar in Figure 11. The Bernoulli-Euler expression {8} is known to error in beams when shear stresses are sufficient to cause non-planarity called warpage in deformed sections. It was argued earlier that shear stresses in the entering span should be small because of the aspect ratio chosen. Since the MD deformations across the web width are planar in the free span in Figure 11 this argument is validated. However the distribution of the friction forces between the web and roller which react the moment are not necessarily linear and will be examined next.

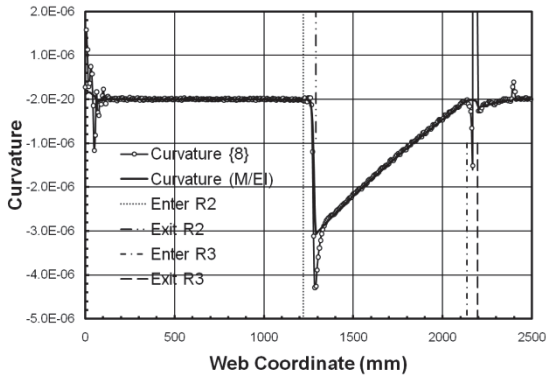

(a)

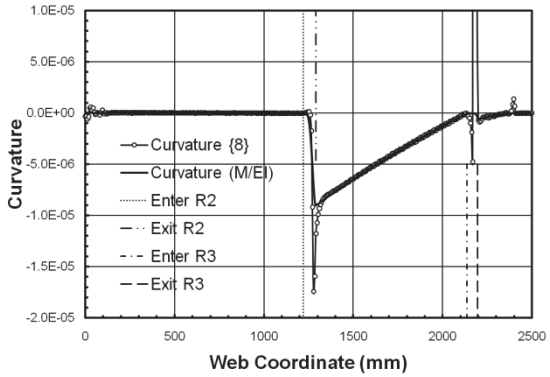
1.0E-05
5.0E-06
0.0E+00
-5.0E-06
-1.0E-05
-1.5E-05
-2.0E-05
Curvature
Curvature {8}
Curvature (M/EI)
Enter R2
Exit R2
Enter R3
Exit R3
0
500
1000
1500
2000
2500
Web Coordinate (mm)

(b)

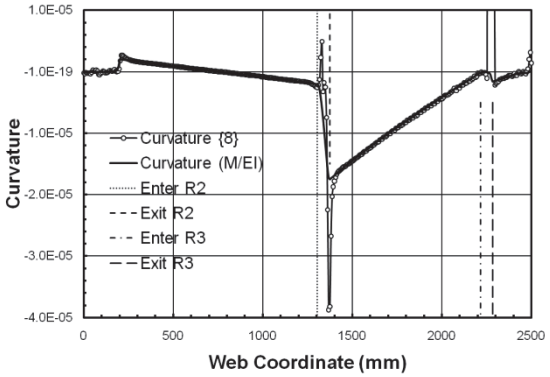
1.0E-05
-1.0E-19
-1.0E-05
-2.0E-05
-3.0E-05
-4.0E-05
Curvature
Curvature {8}
Curvature (M/EI)
Enter R2
Exit R2
Enter R3
Exit R3
0
500
1000
1500
2000
2500
Web Coordinate (mm)

(c)

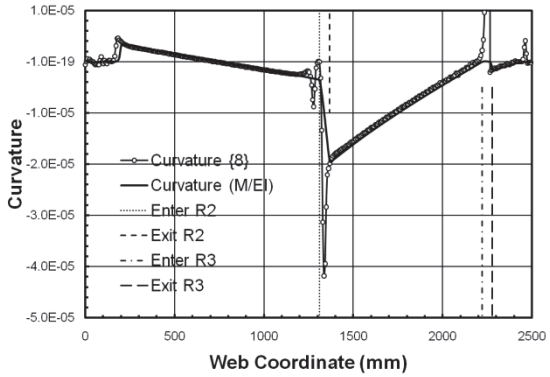
1.0E-05
-1.0E-19
-1.0E-05
-2.0E-05
-3.0E-05
-4.0E-05
-5.0E-05
Curvature
Curvature {8}
Curvature (M/EI)
Enter R2
Exit R2
Enter R3
Exit R3
0
500
1000
1500
2000
2500
Web Coordinate (mm)

(d)

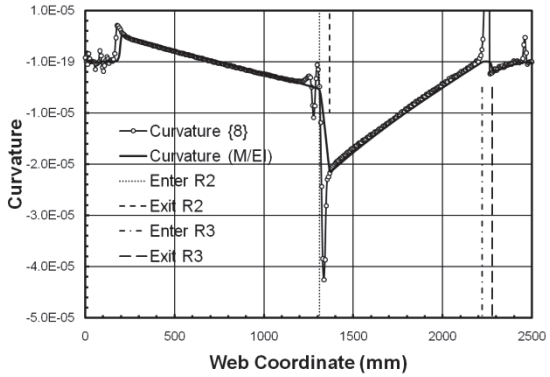

(e)

Figure 10 – Calculated curvature curves for each misaligned angle: (a) 0.074° (b) 0.223° (c) 0.446°, (d) 0.502° and (e) 0.558°

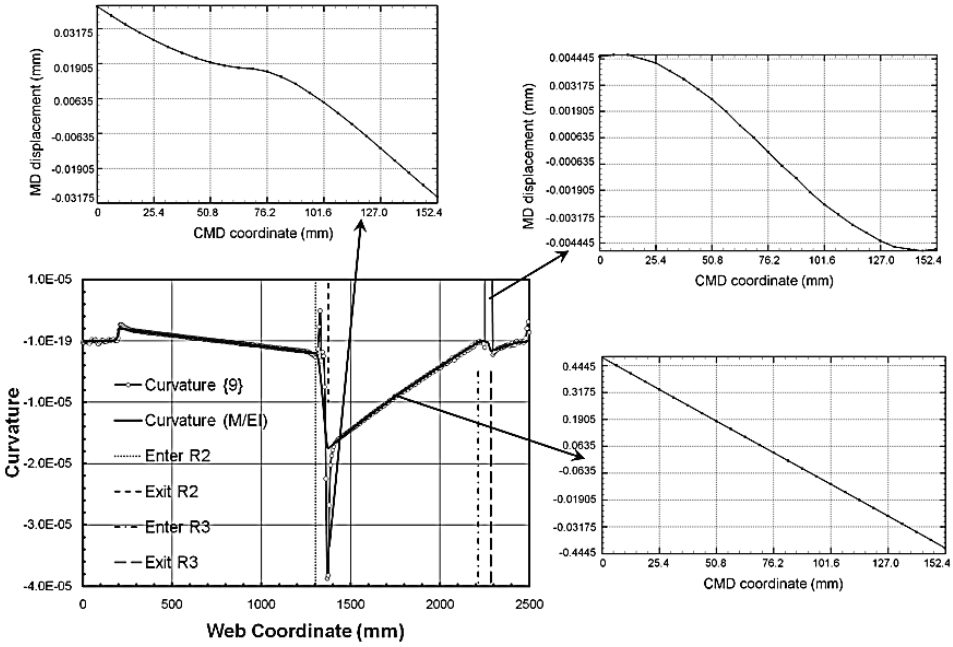

Figure 11 – Curvatures comparison and section shapes at different locations

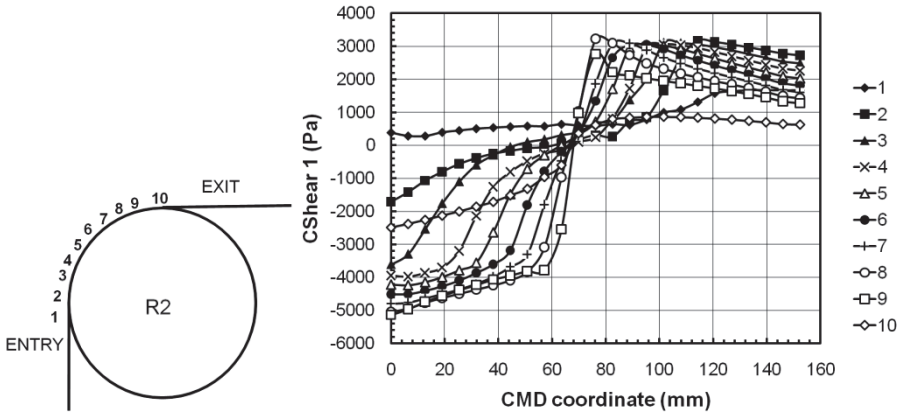

(a) (b)

Figure 12 – CShear 1 stress distribution on R2 from 0.446° misalignment case

As shown in Figure 9 and 10, the misalignment of R3 leads to the upstream moment, which causes web slippage on R2. Due to the frictional contact, the MD frictional shear contact stresses are generated which resist slippage of the web on R2. In Abaqus, the output CShear1 is the contact shear stress between the roller and web along MD. Figure 12 shows the CShear1 stress distribution on R2 for the 0.446° case. CShear1 stresses were harvested from each node of the web contacting roller R2. Figure 12 (a) shows the MD locations of curves in Figure 12 (b) on R2. Figure 12 (b) indicates the Cshear1 stresses along CMD at different MD locations. These distributions of contact shear stress are obviously nonlinear across the web width and are responsible for the non-planar MD deformations that were shown in Figure 11. These contact shear stresses can be integrated to produce the moment (M_{r1}) that is applied to the web by the friction forces in the MD:

$$M_{r1} = \int CShear1 \cdot z \cdot dA_s = \sum_{i=1}^{n} CShear1_i z_i A_{si} \qquad \{10\}$$

where A_{si} is the elemental contact area between the web and roller. Using this expression the moment caused by the web slippage in the MD is calculated to be 0.86 N-m. Since the web slips and rotates on R2, the CMD contact shear stresses also contribute to the reaction moment. In Abaqus, this contact shear stress is defined as CShear2. The moment calculated using CShear2 is about 0.045 N-m. The combined reaction moment due to friction on R2 is 0.905 N-m. Figure 9 (c) shows the calculated moments at the entry and exit point of R2 are about 0.12 N-m and 1.03 N-m, respectively, and the difference of these two is 0.91 N-m which agrees with the calculation using CShear stresses. From Good's closed form solution [3] the moment reacted by friction is:

$$M_r = \frac{\mu TW}{4}\theta = \frac{\mu TW\pi}{8} \qquad \{11\}$$

where θ is the angle of wrap of the web about R2 which is π/2 in this case, W is the web width and μ is the coefficient of friction (0.33). Using expression {11} produces an M_r of

1.14 N-m which is the same moment that Good would have predicted at the exit of R2 when the misalignment of R3 was 0.446°, thus moment transfer into the upstream span should have just begun. Expression {11} produces a moment that can be reacted by friction that is 26% higher than that calculated from Abaqus. This error is offset somewhat in that by allowing no slippage at the exit of R2 Good predicts a moment at that location (1.14 N-m) which is 10.7% higher than predicts by Abaqus (1.03 N-m). It is due to this offset of error that the lateral deformations predicted by Good [3] compare so well with the Abaqus results and the test data in Figure 8.

CONCLUSIONS

Explicit finite element simulations have been conducted that prove the value of this method for addressing lateral mechanics problems in web handing. The simulations produced lateral deformations very similar to results produced by the closed form method developed by Good [3] and in lab measurements. The method developed by Good required assumptions of normal entry to rollers R2 and the misaligned roller R3. His method also enforced normal exit of the web from rollers R1 and R2. Good's method [3] also required the assumption that the moment in the web at the entry of R3 is zero per Shelton [1]. Good's method also relies on an expression for the web moment that can be sustained by friction on roller R2. None of these assumptions were enforced in the Abaqus simulations. It could also be argued that the simulations have provided a method for substantiating the assumptions made in the previous analyses. It should also be noted that Good's method did not account for shearing deformation and that the satisfactory agreement was possible between the Abaqus simulations and the test data because span ratios were employed that prevented shear deformation from having a notable effect. Good's assumption of normal exit from roller R2 is obviously not exact as was shown in Figure 8 for all misalignments. But the assumption of normal exit by Good's method did not produce lateral deformations with significant error for this study. The assumption of zero moment at the entry of the misaligned roller [1] is also not exact, but it is extremely close and still considered valid. The moments shown in Figure 10 indicate that zero moment occurs slightly after the web contacts the misaligned roller. Both Shelton [1] and Good [3] incorporate a basic assumption that a web can be modeled as a beam in which plane sections are assumed to remain plane before and after deformation. The curvatures inferred from moment and from second derivatives of lateral deformation shown in Figure 10 indicate that this assumption appears valid in broad areas of the free spans but as the web encounters rollers where slippage occurs these curvatures diverge. Again the lateral deformations predicted by closed form methods such as that of Good [3] agree with the Abaqus simulations. However assuming the web behaves as a beam may not produce acceptable results for all cases.

It has been shown that the Laser Doppler Velocimeters can be used to infer internal moments in the web that match nicely with moments from the simulations. This is the first non-contact measurement of internal moments for webs in free spans and on rollers.

ACKNOWLEDGEMENTS

The authors thank the industrial sponsors of Web Handling Research Center at Oklahoma State University for providing the funding which made all the work possible.

REFERENCES

1. Shelton, J. J., “Lateral Dynamics of a Moving Web,” Ph.D. Dissertation, Oklahoma State University, 1968.
2. Dobbs, J. N. and Dedl, D. M., “Wrinkle Dependence on Web Roller Slip,” Proceedings of the Second International Conference on Web Handling, Oklahoma State University, June 1995.
3. Good, J. K., "Shear in Multispan Web Systems,” Proceedings of the Fourth International Conference on Web Handling, Oklahoma State University, June 1997.
4. Shelton, J. J., “Interaction Between Two Web Spans Because of a Misaligned Downstream Roller,” Proceedings of the Eighth International Conference on Web Handling, Oklahoma State University, June 2005.
5. Reddy, A., “Analysis of Moment transfer in Multi-span Web Systems,” M.S. Thesis, Oklahoma State University, 2010.
6. Beisel, J. A., “Single Span Web Buckling Due to Roller Imperfections in Web Process Machinery,” Ph.D. Dissertation, Oklahoma State University, October 2006.
7. Abaqus documentation 6.9-EF, 2010.
8. Good, J.K., Kandadai, B.K., and Markum, R., “A New Method for Measurement of Wound-In-Tension in Webs Wound into Rolls,” Journal of Pulp and Paper Science, V 35, No.1, 2009, pp. 17-23.

Explicit Analysis of the Lateral Mechanics of Web Spans	**B. Fu, R. Markum, A. Reddy, S. Vaijapurkar & J. K. Good,** Oklahoma State University, USA

Name & Affiliation	**Question**
Dilwyn Jones, Emral Ltd.	I thought this was very nice work. I have a question about the mesh you used. How many elements were used and how did the size of the element compare with the length of wrap on each roller?
Name & Affiliation	**Answer**
Boshen Fu, Oklahoma State University	My elements were 0.25 inches square. This mesh size was shown to provide a converged result.
Name & Affiliation	**Question**
Keith Good, Oklahoma State University	Boshen, how long did the computation take with that mesh density?
Name & Affiliation	**Answer**
Boshen Fu, Oklahoma State University	Less than two days.
Name & Affiliation	**Question**
Günther Brandenburg, Technische Universität München	If you neglect the bending of a thread or bend, you get a system of first order if you change the angle of misalignment. What is the physical reason for the effect as Shelton has shown that with bending that this model is of second order?
Name & Affiliation	**Answer**
John Shelton, Oklahoma State University	It's the curvature of the web due to the moments that cause the web to curve to make it second order.